Original Article

Densification of matrix graphite for spherical fuel elements used in molten salt reactor via addition of green pitch coke

Zhao He [a, b, c], Hongchao Zhao [a], Jinliang Song [d], Xiaohui Guo [a], Zhanjun Liu [a, b, *], Yajuan Zhong [d, **], T. James Marrow [c]

[a] Key Laboratory of Carbon Materials, Institute of Coal Chemistry, Chinese Academy of Sciences, Taiyuan, 030001, China
[b] Center of Materials Science and Optoelectronics Engineering, University of Chinese Academy of Sciences, Beijing, 100049, China
[c] Department of Materials, University of Oxford, Oxford, OX1 3PH, UK
[d] Shanghai Institute of Applied Physics, Chinese Academy of Sciences, Shanghai, 201800, China

ARTICLE INFO

ABSTRACT

Green pitch coke with an average particle size of 2 μm was adopted as densifier and added to the raw materials of conventional A3-3 matrix graphite (MG) to prepare modified A3-3 matrix graphite (MMG) by the quasi-isostatic molding method. The structure, mechanical and thermal properties were assessed. Compared with MG, MMG had a more compact structure, and exhibited improved properties of higher mechanical strength, higher thermal conductivity and better molten salt barrier performance. Notably, under the same infiltration pressure of 5 atm, the fluoride salt occupation of MMG was only 0.26 wt%, whereas it was 15.82 wt% for MG. The densification effect of green pitch coke endowed MMG with improved properties for potential use in the spherical fuel elements of molten salt reactor.

1. Introduction

Molten salt reactor (MSR), one class of Generation IV advanced reactors, is anticipated to play a vital role in future nuclear fission energy systems. MSR can be liquid-fueled or solid-fueled [1]. In liquid-fueled MSR, a molten fluoride salt mixture bearing fissile material not only acts as the primary nuclear reactor coolant, but also the nuclear fuel [2]. In solid-fueled MSR, a molten fluoride salt mixture is the primary coolant with a solid fuel [2]. Spherical solid fuel elements were originally developed for the high-temperature gas-cooled reactor (HTGR) and are composed of tri-structural isotropic fuel particles distributed in a matrix graphite [3]. In the solid-fueled MSR, the matrix graphite must come into direct contact with the coolant, and so must be resistant to infiltration by the molten fluoride salt mixture. This requires the pore diameter of the matrix graphite to be less than 1 μm [4–6]. Conventional A3-3 matrix graphite (MG) has been used as the matrix graphite for

spherical fuel elements in HTGR, and it might be used as the matrix graphite for fuel elements in solid-fueled MSR. However, as the median pore diameter of MG is approximately 1 μm, with many larger pores, molten salt infiltration may occur. Therefore, it is necessary to improve its molten salt barrier property.

Previous studies have shown that precursor impregnation pyrolysis (PIP) and vapor deposition are two effective methods to improve the barrier property of graphite to molten salt [7–15]. However, these two methods have significant limitations. For example, it is difficult with the PIP method to ensure uniformity of the graphite structure, leading to inhomogeneity of impregnation. Protective coatings prepared by vapor deposition are not only costly, but it is also difficult to guarantee their durability and effectiveness in molten salt environments due to the risk of cracking and peeling. Another traditional method is feasible to improve the molten salt barrier property of graphite, in which preparing high-density graphite consists in incorporating with the mixture of coke and pitch such filler materials as micronized dust particles of carbon or graphite, of carbon black, and so on [16]. A recent study has shown that the solid-phase densification method, in which mesocarbon microbeads (MCMBs) are adopted as a densifier and mixed with the raw materials of MG, is an effective way to densify MG for improved molten salt barrier property [17]. The

beneficial densification effect of MCMBs is mainly due to their self-sintering activity and shrinkage during heat treatment. However, high cost due to low yield and a complicated preparation process greatly limit the potential application of MCMBs, which makes it is very important to find a simpler and lower cost densifier. Green pitch coke, which has similar properties to MCMBs, has low cost and is readily available, and so is a promising candidate.

In this work, green pitch coke with an average particle size of 2 μm was used to densify MG in the preparation of a modified A3-3 matrix graphite (MMG). The microstructures and properties of MG and MMG were investigated and compared, in particular the molten fluoride salt and mercury infiltration behaviors. The densification mechanism was elucidated and analyzed based on the characteristics of green pitch coke.

2. Experimental

2.1. Materials

Both natural graphite and artificial graphite (graphitized coke) with an average particle size of 20 μm were provided by Qingdao Risheng Graphite Co., Ltd, (Shangdong Province, China) and the phenolic resin binder was provided by Shengquan New Material Co., Ltd., (Shandong Province, China). The green pitch coke with an average particle size of 2 μm was prepared in our laboratory by a pressure-assisted semi-carbonization process [18]. The basic properties and group compositions of the green pitch coke were reported in previous work [19]. FLiNaK salt (46.5% LiF-11.5% NaF-42% KF, mole ratio), one potential coolant for MSR [20], was adopted as the impregnation salt.

2.2. Sample preparation

The raw materials of MG are a mixture of natural graphite (64 wt %), artificial graphite (16 wt%) and phenolic resin (20 wt%). Based on the fundamental formula of MG, 15 wt% green pitch coke was added as a raw material to produce MMG. The phenolic resin was dissolved in absolute ethanol (volume ratio 2:1) to form the binder. After kneading, drying, crushing and sieving, the mixtures were converted into resinated powders [21], which were put into silicone molds to form spherical green bodies at 250 MPa pressure by the quasi-isostatic molding method. After carbonization at 800 °C for 4 h and purification at 1950 °C for 1 h, these two kinds of matrix

Fig. 1. As-prepared graphite samples in this work.

graphite (MG and MMG) were obtained. And the as-prepared graphite samples are shown in following Fig. 1.

2.3. Sample characterization methods

The Archimedes method was used to measure sample density. An automatic mercury porosimeter (AutoPore IV 9500) measured the pore structural information of sample. X-ray diffraction (XRD, Bruker D8 Advance, λ = 0.15406 nm) and Raman spectroscopy (HORIBA Jobin-Yvon, LabRam HR800, λ = 514 nm) were applied to characterize the crystal structures of sample. A field emission scanning electron microscope (SEM, JSM-7001F) was used to characterize the sample microstructure. The three-point bending method and standard of ASTM C695-91 [22] were adopted to test the flexural strength and the compressive strength of sample, respectively. The laser flash technique (Nano Flash Apparatus, LFA 447/2-2, NETZSCH) measured the thermal diffusivity and a differential scanning calorimeter (DSC, 200F3, NETZSCH) measured the specific heat, so equation (1) could be used to calculate the thermal conductivity (k),

$$k = a \times C_p \times \rho \tag{1}$$

where a, C_p and ρ refer to thermal diffusivity, specific heat and density, respectively. A dilatometer (Netzsch DIL 402 PC, NETZSCH) tested the coefficient of thermal expansion (CTE) and the anisotropy factor (ϕ) was calculated via equation (2),

$$\phi = \alpha_\perp \big/ \alpha_{||} \tag{2}$$

where $\alpha_\perp$ and $\alpha_{||}$ are the CTEs perpendicular and parallel to the molding pressure, respectively.

Molten salt infiltration experiments were carried out following the experimental process that has been reported by our previous works [9,10]. The infiltration experiments were conducted at 650 °C under argon with an infiltration time of 12 h under different infiltration pressures (1, 2, 3, 4 and 5 atm). The weight gain ratio (η, wt %) for each graphite sample (namely its infiltration amount of molten salt) was obtained using Equation (3),

$$\eta = (m_2 - m_1)/m_1 \tag{3}$$

where m_1 and m_2 refer to the sample weight before and after the molten salt infiltration experiment, respectively.

3. Results and discussion

3.1. Microstructures and thermo-physical properties of MG and MMG

Table 1 summarizes the measured properties of the MG and MMG samples and shows that the introduction of the green pitch coke as densifier has improved the properties of MMG compared to MG. The bulk density increased from 1.68 g/cm³ for MG to 1.74 g/cm³ for MMG, and the median pore diameter and porosity reduced from 1.050 μm and 23.2% for MG to 0.676 μm and 18.6% for MMG, respectively. The compressive and flexural strengths increased, together with increased thermal conductivity. Fractography of these two graphites (Fig. 2) demonstrates the greater compactness of MMG. Specifically, there are some large pores in MG (labeled by yellow arrows in Fig. 2a), whereas only small pores exist in MMG (Fig. 2b).

Although phenolic resin derived carbon is difficult to graphitize, both MG and MMG have obvious graphitic structures (Fig. 3), which can be ascribed more to their graphitic filler particle content than

Table 1
Properties of MG and MMG.

Property	MG	MMG
Green body density (g/cm^3)	1.75 ± 0.01	1.78 ± 0.01
Mass loss rate during HTP (%)	10.22 ± 0.02	10.15 ± 0.02
Volume shrinkage rate during HTP (%)	6.43 ± 0.03	8.09 ± 0.02
Bulk density (g/cm^3)	1.68 ± 0.01	1.74 ± 0.01
Median pore diameter (μm)	1.050 ± 0.025	0.676 ± 0.031
Porosity (%)	23.2 ± 0.2	18.6 ± 0.2
Compressive strength (MPa)	45.8 ± 2.1	54.5 ± 1.8
Flexure strength (MPa)	22.7 ± 1.8	26.7 ± 1.5
L_c(nm)	21.6 ± 0.1	21.8 ± 0.1
Graphitization degree (%)	86.1 ± 0.2	86.3 ± 0.2
Thermal conductivity (25 °C, W m^{-1} K^{-1})	59.7 ± 1.4	64.2 ± 1.5
CTE (298–973 K, 10^{-6}/K)	3.51 ± 0.02	3.67 ± 0.02
Anisotropic factor	1.02 ± 0.01	1.02 ± 0.01

Note: HTP=Heat treatment process including carbonization and purification.

phenolic resin derived carbon. The XRD spectra (Fig. 3a and b) are very similar and show close crystallographic parameters. The graphitization degree (g) was calculated according to equation (4),

$$g = \frac{0.3440 - d_{002}}{0.3440 - 0.3354} \tag{4}$$

where interlayer spacing d_{002} for MG is 0.336593 nm and 0.336580 nm for MMG, so the graphitization degrees of MG (86.1%) and MMG (86.3%) are quite close. The mean dimension of crystallites perpendicular to the diffracting plane (002) L_c was calculated according to the Scherrer equation,

$$L_c = \frac{0.9\lambda}{\beta_{002} cos\theta_{002}} \tag{5}$$

where β_{002} is diffraction peak width and θ_{002} the Bragg angle. For MG, L_c is 21.6 nm, which is also quite close to 21.8 nm for MMG. Typical Raman spectra of MG and MMG are shown in Fig. 3c. The D band and G bands at about 1350 cm^{-1} and 1580 cm^{-1} respectively represent the first-order defect-induced Raman features and the doubly degenerate phonon mode with E$_{2g}$ symmetry for a sp^2 carbon network. The ratio I$_D$/I$_G$ (the intensity ratio of D band and G band) can also be adopted to judge the graphitization degree [23], and the similar I$_D$/I$_G$ for MG (0.38) and MMG (0.37) also indicates their similar graphitization degrees.

There are two main reasons for the improvement of the compactness of matrix graphite after the introduction of green pitch coke as a densifier. First, the fine green pitch coke particles filled the interstices between larger filler particles (natural graphite

and artificial graphite). This increased the green body density during the molding process, which is conducive to the increase of the density of resulting matrix graphite. Secondly, with the introduction of green pitch coke particles, the volume shrinkage rate of the green bodies during heat treatment process increased from 6.43% to 8.09%, which is also conducive to increased density. The more compact structure of MMG is the main reason for its higher mechanical strength, higher thermal conductivity and higher CTE, as both MG and MMG have very similar graphitization degree. The anisotropy factors are both 1.02, which indicates that the introduction of fine green pitch coke as densifier has no influence on this herein. Low anisotropy is conducive to ensuring the structural integrity and service life of graphite in the MSR irradiation environment.

High thermal conductivity and low CTE are two key properties for the matrix graphite in solid-fueled MSR, in order to enhance the heat exchange between the fuel elements and the coolant, to reduce thermal stresses and to enhance the fuel structural integrity [23,24]. The variation of thermal properties with temperature of MG and MMG are summarized in Fig. 3. With increasing temperature, the thermal conductivities of both graphites decrease (Fig. 4a), which is due to the decrease of phonon motion mean free path and the increase of phonon scattering intensity [25]. Specifically, the thermal conductivity of MG decreased from 59.7 W m^{-1} K^{-1} at 25 °C to 15.3 W m^{-1} K^{-1} at 800 °C, whereas the thermal conductivity of MMG decreased from 64.2 W m^{-1} K^{-1} at 25 °C to 16.2 W m^{-1} K^{-1} at 800 °C. The higher thermal conductivity of MMG can be ascribed to its more compact structure. In a previous study, where MCMB densifier was used with the same average particle size as the green pitch coke of this study, the thermal conductivity of the densified matrix graphite was slightly lower than that of raw matrix graphite [17]. This indicates that green pitch coke may have some advantage over MCMBs as a densifier for the matrix graphite. The thermal expansion curves (Fig. 4b) show that for MMG, the CTE between 25 °C and 700 °C is 3.67 × 10^{-6} K^{-1}, which is higher than the 3.51 × 10^{-6} K^{-1} of MG, and this can be ascribed to the more compact structure of MMG than MG. Although the CTE of MMG increased with its improved densification, the MMG still meets the maximum CTE requirement (5.50 × 10^{-6} K^{-1}) for matrix graphite for spherical fuel elements in the solid-fueled MSR [17], and is much lower than the 6.01 × 10^{-6} K^{-1} to 6.15 × 10^{-6} K^{-1} of matrix graphite derived from pure MCMBs [26] and 3.94 × 10^{-6} K^{-1} of matrix graphite densified by MCMBs with the same average particle size as the green pitch coke used in this experiment [17].
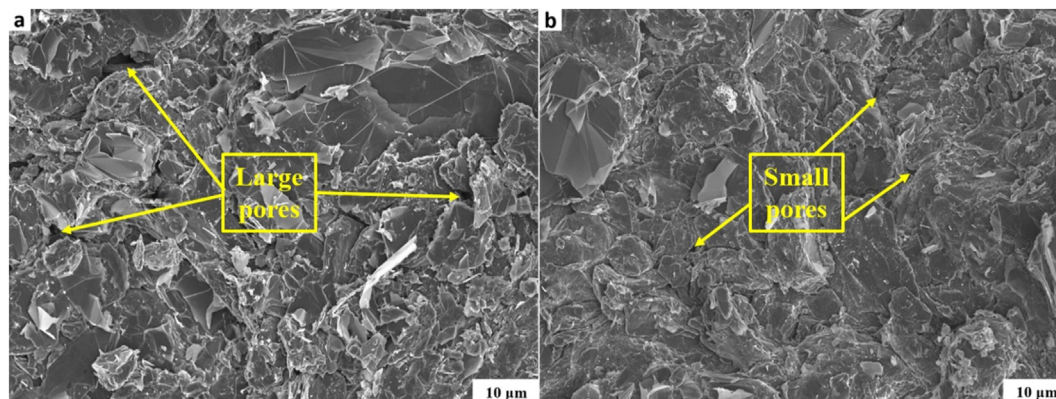
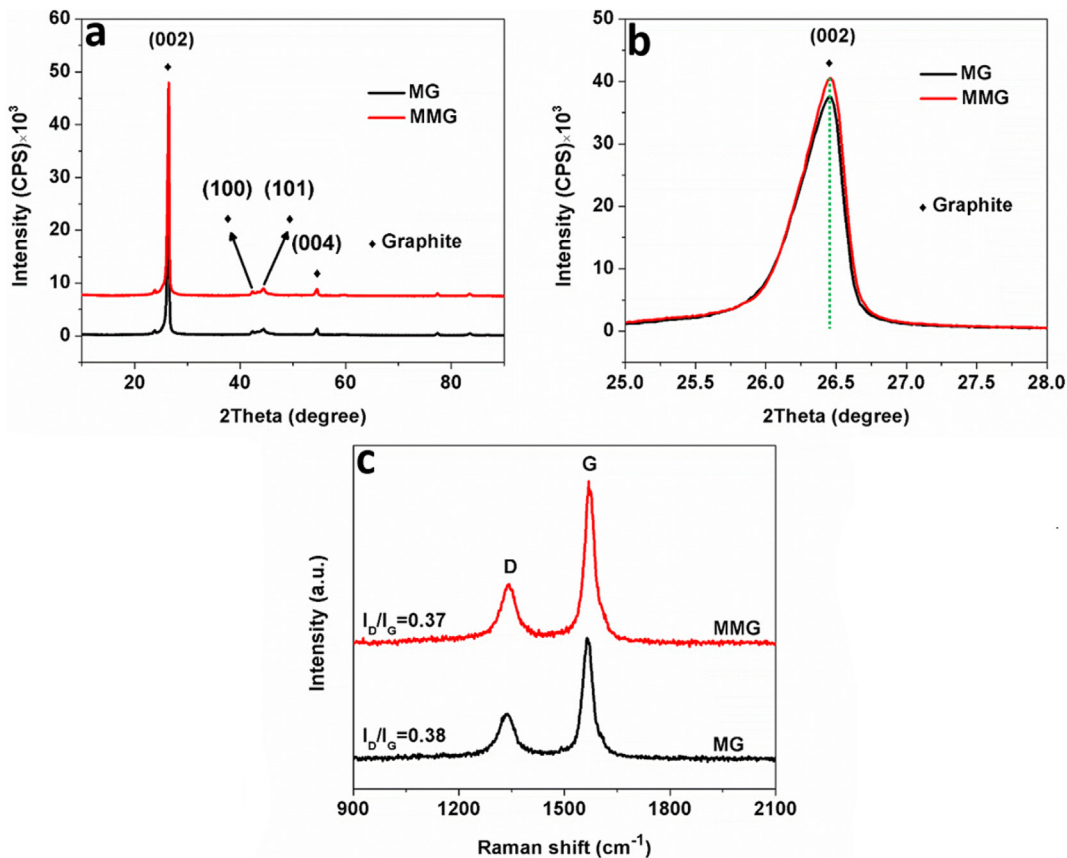**Fig. 2.** Fracture surface SEM images of MG (a) and MMG (b).

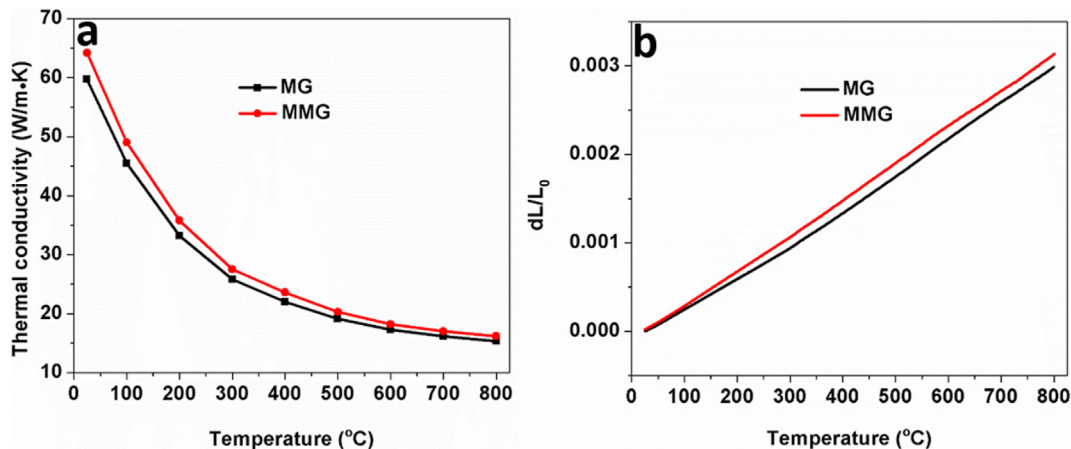**Fig. 3.** XRD spectra (a, b) and Raman spectra (c) of MG and MMG.

Fig. 4. Thermal conductivity (a) and representative thermal expansion (b) curves of MG and MMG.

3.2. Mercury and molten salt infiltration into MG and MMG

Fig. 5a−b shows the pore size distributions and mercury infiltration curves of these two matrix graphites. The data are consistent with the greater compactness of MMG than MG. The mercury infiltration process is composed of three stages (Fig. 5b). For MG, mercury did not infiltrate significantly when the infiltration pressure was less than the threshold pressure of 9.83×10^5 Pa (first stage), but when the infiltration pressure was between 9.83×10^5 Pa and 2.88×10^6 Pa (second stage) mercury could infiltrate significantly. When the infiltration pressure exceeded 2.88×10^6 Pa (third stage), a small quantity of mercury could also infiltrate new pores that derived from the rupture of fragile closed pores [27]. For MMG, the threshold pressure of 1.49×10^6 Pa is higher than that of MG, due to its much smaller median pore diameter (Table 1). The total mercury infiltration of MMG is
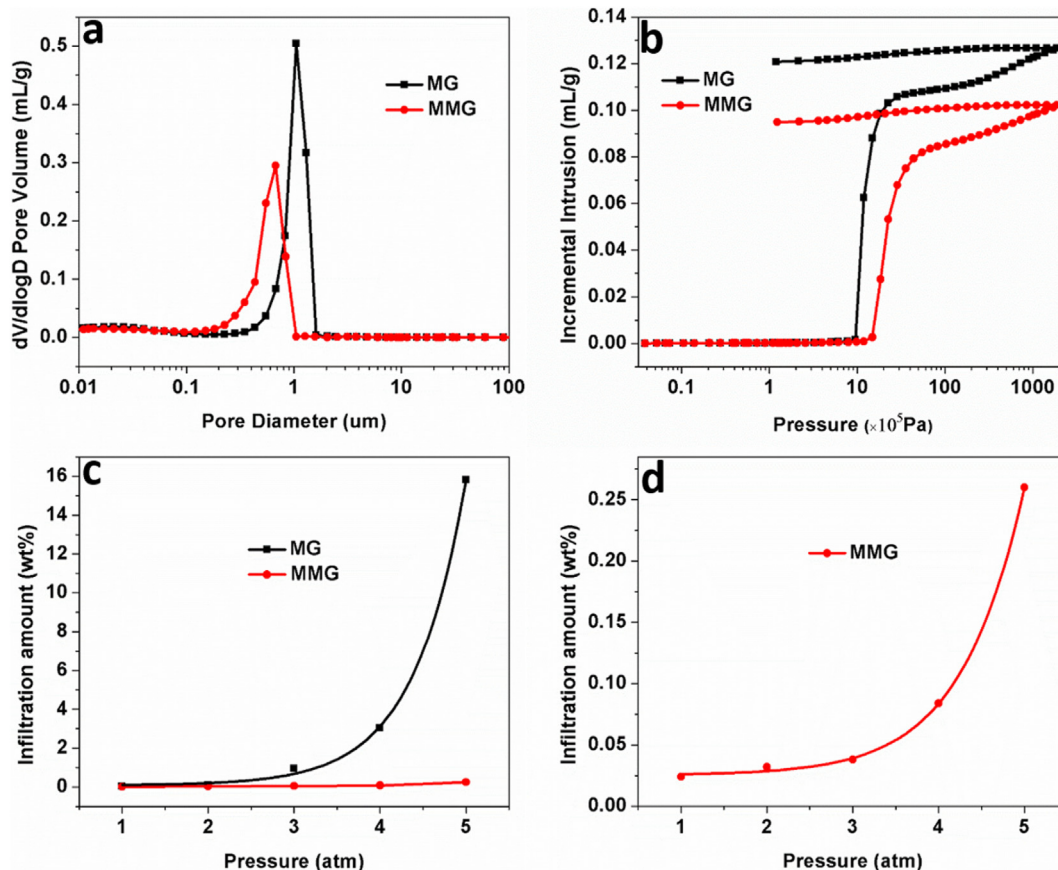
Fig. 5. Pore diameter distributions (a), mercury infiltration (b) and molten salt infiltration (c) curves of MG and MMG. The data for MMG are replicated in (d) for greater clarity.

0.1023 ml g^{-1}, less than that of MG (0.1268 ml g^{-1}), which is consistent with the lower porosity of MMG.

Fig. 5c–d shows the molten salt infiltration curves for the two graphites. Molten salt could infiltrate into MG much more significantly than MMG once the infiltration pressure exceeded 3 atm, reaching to 15.82 wt% under 5 atm. In comparison, MMG exhibited a much lower molten salt infiltration of only 0.25 wt%, even under 5 atm pressure. The infiltration behaviors of mercury and molten FLiNaK salt into graphite can be compared due to their similar non-wetting [26] by using a scaling factor (X) that is based on the Washburn equation [28],

$$\Delta P = -\frac{4\gamma cos\theta}{\delta} \tag{6}$$

where ΔP, γ, θ and δ refer to the capillary pressure, surface tension, contact angle and pore size, respectively. For the same graphite sample, X can be defined as [29],

$$X = \frac{\Delta P_{Hg}}{\Delta P_{Salt}} = \frac{\gamma_{Hg}cos(\theta_{Hg})}{\gamma_{Salt}cos(\theta_{Salt})} \tag{7}$$

where for the graphite and mercury, γ_{Hg} and θ_{Hg} are about

485 dyne/cm and 130°, respectively [30] and for the graphite and molten FLiNaK salt system, γ_{Salt} and θ_{Salt} are about 160 dyne/cm and 140°, respectively [31]. The obtained scaling factor, X, is 2.54, so the threshold pressures of molten salt, calculated for MG and MMG from their corresponding threshold pressures of mercury (Table 2), are consistent with the experimental thresholds of 3 atm and >5 atm, respectively. The relative resistance to salt infiltration is further demonstrated by fractography of the infiltrated graphite (Fig. 6). Specifically, white salt particles fill the pores of MG (Fig. 6a), whereas no obvious salt particles are observed within MMG (Fig. 6b). The maximum operation pressure of a solid-fueled MSR is 0.5 MPa [32], so the improved molten barrier property of MMG make it quite suitable for the matrix graphite for spherical fuel elements to be used in a solid-fueled MSR.

4. Conclusions

The feasibility of densification of matrix graphite by introduction of green pitch coke with an average particle size of 2 μm as densifier has been demonstrated, and the microstructure and overall properties of the matrix graphite were improved. Specifically, the as-prepared MMG exhibited smaller median pore diameter, lower porosity, higher mechanical strength, higher thermal conductivity and better molten salt barrier property than MG. The threshold pressure for molten salt infiltration for MMG is higher than the maximum operation pressure of solid-fueled MSR, which indicates MMG has great potential to be applied in these systems. Furthermore, the densification process should have effect on the irradiation properties of graphite, which will be elucidated in our future work.
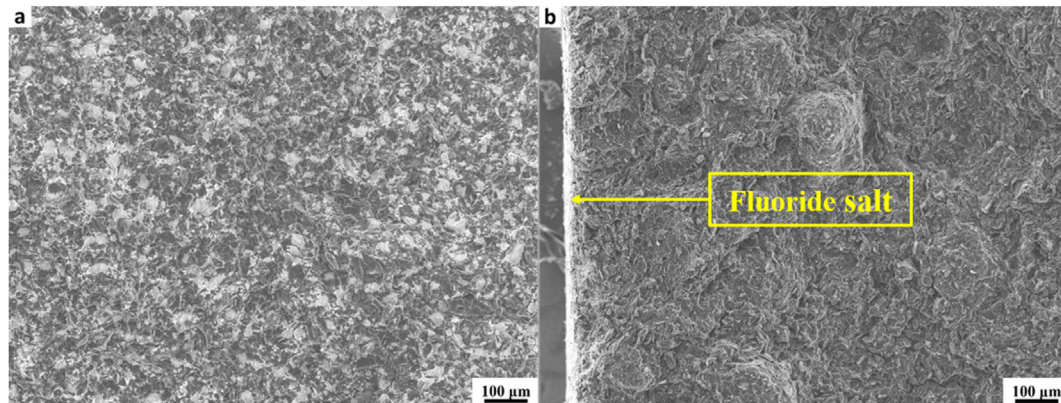
Table 2
Threshold pressure in Mercury (measured) and molten FLiNaK salt (predicted).

Threshold pressure	MG	MMG
Mercury	9.83×10^5 Pa	1.49×10^6 Pa
Molten FLiNaK salt	3.87×10^5 Pa (3.82 atm)	5.87×10^5 Pa (5.79 atm)

Fig. 6. Fracture surface SEM images of infiltrated graphite samples tested at 5 atm: MG (a) and MMG (b).

Declaration of competing interest

We have no conflict of interest to declare.

Acknowledgments

References

[1] Z. Dai, Thorium molten salt reactor nuclear energy system (TMSR), Molten Salt Reactors and Thorium Energy (2017) 531–540.
[2] J. Uhlíř, Chemistry and technology of molten salt reactors – history and perspectives, J. Nucl. Mater. 360 (1) (2007) 6–11.
[3] Advances in High Temperature Gas Cooled Reactor Fuel Technology, Vienna. IAEA-TECDOC-CD-1674, Austria, 2012.
[4] R.B. Briggs, P.R. Kasten, Molten-salt Reactor Program Semiannual Progress Report, Oak Ridge National Laboratory, ORNL-3419, USA, 1963, pp. 71–73.
[5] H. Mccoy, R. Beatty, W. Cook, et al., New developments in materials for molten salt reactors, Nucl. Appl. Technol. 8 (2) (1970) 156–169.
[6] M.W. Rosenthal, P.N. Haubenreich, R.B. Briggs, The Development Status of Molten-Salt Breeder Reactors, Oak Ridge National Laboratory, ORNL-4812, USA, 1972, pp. 273–290.
[7] P.R. Kasten, E.S. Bettis, W.H. Cook, et al., Graphite behavior and its effects on MSBR performance, Nucl. Eng. Des. 9 (2) (1969) 157–195.
[8] V. Bernardet, S. Gomes, S. Delpeux, et al., Protection of nuclear graphite toward fluoride molten salt by glassy carbon deposit, J. Nucl. Mater. 384 (3) (2009) 292–302.
[9] Z. He, P. Lian, Y. Song, et al., Improving molten fluoride salt and Xe^{135} barrier property of nuclear graphite by phenolic resin impregnation process, J. Nucl. Mater. 499 (2018) 79–87.
[10] Z. He, P. Lian, Y. Song, et al., Protecting nuclear graphite from liquid fluoride salt and oxidation by SiC coating derived from polycarbosilane, J. Eur. Ceram. Soc. 38 (2) (2018) 453–462.
[11] Z. He, J. Song, P. Lian, et al., Excluding molten fluoride salt from nuclear graphite by SiC/glassy carbon composite coating, Nucl. Eng. Techno. 51 (5) (2019) 1390–1397.
[12] S. Feng, L. Xu, L. Li, et al., Sealing nuclear graphite with pyrolytic carbon, J. Nucl. Mater. 441 (1–3) (2013) 449–454.
[13] X.J. He, J.L. Song, L. Xu, et al., Protection of nuclear graphite toward liquid fluoride salt by isotropic pyrolytic carbon coating, J. Nucl. Mater. 442 (1–3) (2013) 306–308.
[14] X.J. He, J.L. Song, J. Tan, et al., SiC coating: an alternative for the protection of nuclear graphite from liquid fluoride salt, J. Nucl. Mater. 448 (1–3) (2014) 1–3.
[15] J.L. Song, Y.L. Zhao, X.J. He, et al., Preparation of pyrolytic carbon coating on graphite for inhibiting liquid fluoride salt and Xe^{135} penetration for molten salt breeder reactor, J. Nucl. Mater. 456 (2015) 33–40.
[16] René Blachard, Saint-Martin-le-Vinoux, Louis Bochirol, et al., Process for the Densification of Carbonaceous Bodies, U.S. Patent 3321327, 1967.
[17] H. Wang, L. Xu, Y. Zhong, et al., Mesocarbon microbead densified matrix graphite A3-3 for fuel elements in molten salt reactors, Nucl. Eng. Techno. 53 (5) (2021) 1569–1579.
[18] H. Zhao, Z. He, Z. Liu, et al., Self-sintered nanopore-isotropic graphite derived from green pitch coke for application in molten salt nuclear reactor, Ann. Nucl. Energy 131 (2019) 412–416.
[19] H.-c. Zhao, Z. He, X.-h. Guo, et al., Effect of the average grain size of green pitch coke on the microstructure and properties of self-sintered graphite blocks, N. Carbon Mater. 35 (2) (2020) 184–192.
[20] B.A. Frandsen, S.D. Nickerson, A.D. Clark, et al., The structure of molten FLiNaK, J. Nucl. Mater. 537 (2020).
[21] R.E. Schulze, H.A. Schulze, W. Rind, Graphitic Matrix Materials for Spherical HTR Fuel Elements, Jül-Spez-167, 1982, pp. 3–5.
[22] ASTM C695-91, Standard Test Method for Compressive Strength of Carbon and Graphite, 2010.
[23] S. Xu, F. Kang, Carbon and Graphite Materials in Nuclear Engineering, vol. 204, Tsinghua University Press, Beijing (China), 2010, pp. 234–242.
[24] X. Zhou, Z. Lu, J. Zhang, et al., Study on the comprehensive properties and microstructures of A3-3 matrix graphite related to the high temperature purification treatment, Sci. Technol. Nuc. Ins. 2018 (2018) 1–10.
[25] S. Chakraborty, D. Debnath, A.R. Mallick, et al., Microscopic, mechanical and thermal properties of spark plasma sintered ZrB$_2$ based composite containing polycarbosilane derived SiC, Int. J. Refract. Metals Hard Mater. 52 (2015) 176–182.
[26] Y. Zhong, J. Zhang, J. Lin, et al., Mesocarbon microbead based graphite for spherical fuel element to inhibit the infiltration of liquid fluoride salt in molten salt reactor, J. Nucl. Mater. 490 (2017) 34–40.
[27] Pore Size Distribution and Porosity of Solid Materials by Mercury Porosimetry and Gas Adsorption-Part 1: Mercury Porosimetry, 2005, p. 1. GB/T 21650.1-2008/ISO15901-1.
[28] E.W. Washburn, The dynamics of capillary flow, Phys. Rev. 17 (3) (1921) 273–283.
[29] Z. He, L. Gao, W. Qi, et al., Molten FLiNaK salt infiltration into degassed nuclear graphite under inert gas pressure, Carbon 84 (2015) 511–518.
[30] A. Awasthi, Y.J. Bhatt, S.P. Garg, Measurement of contact angle in systems involving liquid metals, Meas. Sci. Technol. 7 (5) (1996) 753–757.
[31] P. Lian, J. Song, Z. Liu, et al., Preparation of ultrafine-grain graphite by liquid dispersion technique for inhibiting the liquid fluoride salt infiltration, Carbon 102 (2016) 208–215.
[32] H.-X. Xu, J. Lin, Y.-J. Zhong, et al., Characterization of molten 2LiF–BeF$_2$ salt impregnated into graphite matrix of fuel elements for thorium molten salt reactor, Nucl. Sci. Tech. 30 (5) (2019).